Int. J. Heat Mass Transfer. Vol. 30, No. 8, pp. 1693–1702, 1987
Printed in Great Britain

0017–9310/87 $3.00+0.00

A distributed model for liquid-phase heat transfer in fixed beds

D. J. GUNN and M. N. SABRI
Department of Chemical Engineering, University College of Swansea, Singleton Park, Swansea SA2 8PP, U.K.

(*Received* 2 *September* 1986 *and in final form* 26 *January* 1987)

Abstract—Although the representation of gas-phase heat transfer by distributed models is now established, corresponding examinations of distributed models for liquid-phase heat transfer have not been reported. In this work liquid flowing through fixed beds of particles was heated at the wall of the bed and the temperature distribution was measured at the end of the bed by an array of thermocouples. The experimental temperature distribution was compared with the predicted temperature distribution for two models of heat transfer in the fixed bed. In the first model heat transfer was assumed to take place by radial and axial thermal dispersion and axial convection with a thermal resistance at the wall taken to represent changes in porosity and conductivity near the wall. In the second model the same model for heat transfer was taken to hold in the bulk region, but a variation in thermal properties was considered to extend over a fraction of a particle diameter from the wall. For heat transfer to small particles and to particles of high thermal conductivity both models represented the experimental data equally well within the range of Reynolds number from 5 to 1000. However, for large particles of low thermal conductivity the two-region model gave a significantly better representation of the experimental measurements.

INTRODUCTION

ALTHOUGH there are several reported investigations into heat transfer from containing walls to air flowing through fixed beds of particles in which the experimental measurements have been interpreted by means of distributed models, there are no equivalent experiments for heat transfer to liquids. Yet the mechanistic interpretation of heat transfer phenomena in fixed beds is facilitated by such measurements because the change of fluid from air to water corresponds to an order of magnitude increase in the Prandtl number for the fluid, as well as major changes in density, viscosity and thermal conductivity.

In the usual experimental arrangement for measuring heat transfer into fixed beds, the wall is heated and fluid passing through the bed of particles is heated according to the partial differential equation [1]

$$K_L\frac{\partial^2 T}{\partial x^2}+\frac{K_R}{R}\frac{\partial}{\partial R}\left(R\frac{\partial T}{\partial R}\right)-UK_f\frac{\partial T}{\partial x}=0. \quad (1)$$

The boundary conditions to this equation reflect a difference in bed porosity near the wall [2, 3], in which the porosity changes from 1.0 at the wall to a value of 0.37 at a distance from the wall of about $0.3d$ when the particles show small irregularities of shape. When the particle size is small in the domain of the tube the extent of the wall region may be neglected and the boundary conditions at the wall are

$$h(T_0-T)=K_R\frac{\partial T}{\partial R} \quad \text{at} \quad R=R_0, \quad x>0 \quad (2)$$

$$hT=-KR\frac{\partial T}{\partial R} \quad \text{at} \quad R=R_0, \quad x<0 \quad (3)$$

where equations (2) and (3) show that the bed is unheated for negative x and heated for $x>0$. The solution to equation (1) that satisfies continuity of temperature and temperature gradient for $x>0$ has been given by Gunn and Khalid [7]. It is

$$\frac{T}{T_0}=-\sum_{s=1}^{\infty}R_0H\sqrt{K_LK_R}\times\left(\frac{\sqrt{(R_0^2K^2K_L+\beta_s^2K_R)}+R_0K\sqrt{K_L}}{\sqrt{(R_0^2K^2K_L+\beta_s^2K_R)}}\right)\times\frac{J_0(\beta_sR/R_0)}{(R_0^2H^2K_L+\beta_s^2K_L)J_0(\beta_s)}\times\exp\left[x\left(K-\sqrt{\left(K^2+\frac{\beta_s^2K_R}{R_0^2K_L}\right)}\right)\right], \quad x>0 \quad (4)$$

where $H=h/\sqrt{(K_LK_R)}$, $K=K_fU/2K_L$, and β_s are roots of

$$\beta K_RJ_1(\beta)-hR_0J_0(\beta)=0. \quad (5)$$

According to equation (2) there is a temperature jump at the wall, an acceptable condition when the particle size is relatively small since the discontinuity is small and reflects the change in thermal properties near the wall as the porosity is increased. When the particle size is larger, however, the extent of the porosity boundary layer becomes a more significant proportion of the tube cross-section and this condition is recognized by dividing the fixed bed into

NOMENCLATURE

d	diameter of particles	R_1	radius of bulk region
D	molecular diffusivity	R_0	radius of tube
h	wall heat transfer coefficient	Re	Reynolds number, $dU\rho/\mu$
H	$h/\sqrt{(K_L K_R)}$	Sc	Schmidt group, $\mu/(D\rho)$
J_0	Bessel function, zero order, first kind	T	temperature of fluid
K	$K_f U/2K_L$	T_0	temperature of wall
K_f	volumetric thermal capacity of fluid	U	superficial velocity
K_L	axial coefficient of thermal dispersion referred to superficial area	X	axial coordinate.
K_R	radial coefficient of thermal dispersion referred to superficial area	Greek symbols	
Nu	Nusselt number, hd/λ	α	defined by equation (7)
Pe	radial Peclet group, $UK_f d/K_R$	β_s	roots of equation (5)
Pe_f	convective Peclet group defined by equations (12) and (13)	λ	thermal conductivity of fluid
Pr	Prandtl group, $K_f\mu/(\lambda\rho)$	λ_0	thermal conductivity of fixed bed at very low flow rate
R	radial coordinate	μ	viscosity of fluid
		ρ	density of fluid.

two regions. In the inner bulk region the temperature distribution is described by equation (1), and this region extends from $R = 0$ on the axis to $R = R_1$, that from porosity measurements extends to about 0.3 particle diameters from the wall. In the wall region Gunn and Ahmad [4] have considered that the temperature is described by the quadratic expression

$$\frac{T-T_0}{T_1-T_0} = (2-\alpha)\left(\frac{R-R_0}{R_1-R_0}\right)+(\alpha-1)\left(\frac{R-R_0}{R_1-R_0}\right), \quad R_1 \leqslant R \leqslant R_0, \quad x > 0 \quad (6)$$

where

$$\alpha = \left(\frac{\partial T}{\partial R}\right)_1 \frac{R_1-R_0}{T_0-T_0} = \frac{K_R}{T_1-T_0}\left(\frac{\partial T}{\partial R}\right)_1 \times \frac{R_1-R_0}{K_R} = \frac{h(R_0-R_1)}{K_R} \quad (7)$$

so that α is a dimensionless group that characterizes heat transfer in the wall region. Expression (6) ensures continuity of temperature and temperature gradient in the wall and bulk regions.

For this two-region model the temperature within the bulk region is given by equations (4) and (5) with R_1 in place of R_0. Thus the prediction of the two-region model is given by equations (4) and (7) with R_1 in place of R_0 in equation (4), while the prediction of the single region model is equation (4) alone, an expression that will therefore include a temperature discontinuity at $R = R_0$. The temperature distribution and the temperature gradient for the two-region model are continuous over the full extent of the tube.

THE EXPERIMENTAL ARRANGEMENT

A line diagram of the experimental arrangement is shown as Fig. 1. Water from a constant head tank was metered through a bank of three rotameters calibrated over the range from 0.3 to 50 l min^{-1} and thence into a flow distributor at the base of the heat exchanger. A diagram of the heat exchanger that was constructed from 1.5 mm thick brass tube is shown in Fig. 2. Two heat exchangers were employed, one 0.61 m long used for the smallest particles, and the second 1.23 m long. Three steam entries were used, and condensate was removed through three outlets connected to a condensate pump.

After heating, water flowing through the fixed bed of particles entered a concentric arrangement of four polypropylene cylinders that projected 50 mm from the upper surface of the Tufnol flange into the inner brass cylinder so as to touch the top of the packing. The polypropylene cylinders prevented radial mixing, until the temperature of the heated water had been measured by resin-covered chromel–alumel thermocouples. Other thermocouples were used to measure the temperature of the wall and the inlet temperature. Each thermocouple and thermocouple group was connected to a six digit voltmeter by a rotary switch.

The inner brass tube of the heat exchanger was filled with particles under study, 0.5 and 6 mm diameter glass spheres, 10.3 mm diameter nickel spheres, and 25.4 mm diameter polypropylene spheres. Movement of the particles was prevented by a coarse and a fine brass perforated disc secured at the top of the bed.

Water was allowed to flow through the bed to remove air, and steam was then admitted at a pressure between 1.7 and 3.7 bar according to the water flowrate. The temperatures registered by the wall ther-

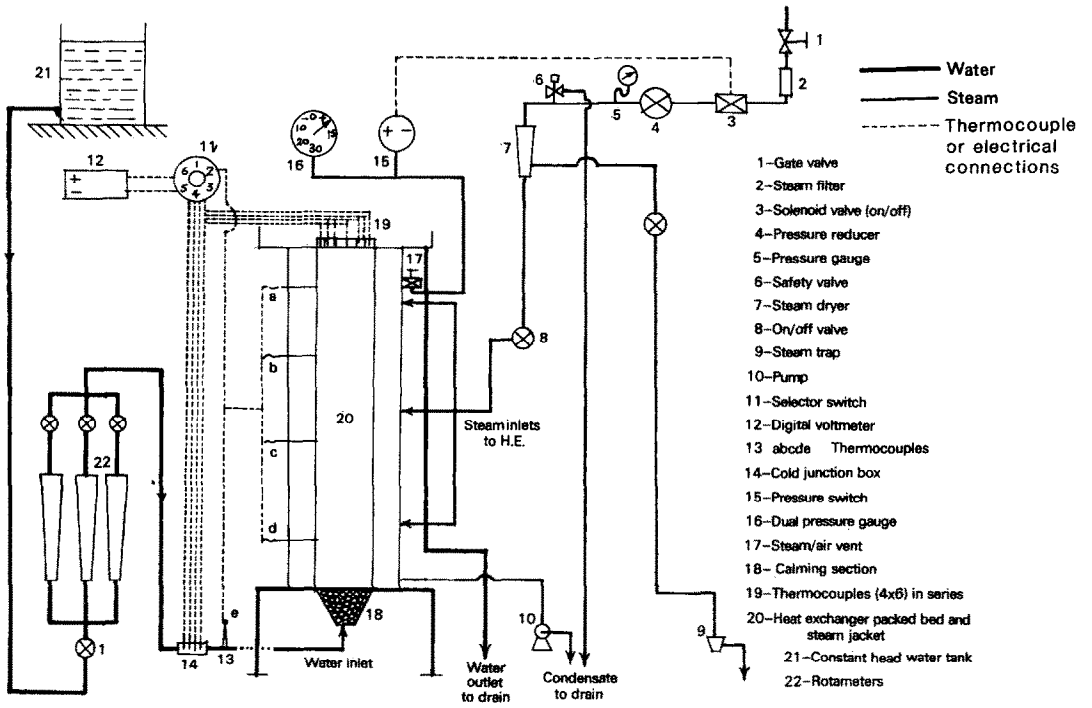

FIG. 1. Line diagram of experimental apparatus.

mocouples remained constant with a variation of ± 0.25°C but less than 90°C to avoid boiling. To avoid superheating the steam on expansion from the steam supply to the annular jacket, the steam trap was disconnected by closing a valve so that steam injection was accompanied by injection of condensate. The wall temperature then corresponded to the saturation temperature of the steam. Thermocouple readings were monitored every 10 min until steady state was reached when all temperatures were recorded.

Temperatures measured at the exit of the bed were converted to temperature ratios formed as

$$\frac{T_{\text{annular}} - T_{\text{ambient}}}{T_{\text{wall}} - T_{\text{ambient}}}.$$

These temperatures were then compared in a computer program with theoretical temperatures for corresponding annuli found by integration of equation (4) over the annulus for the single region model, or by the integration of equations (4) and (6) as appropriate for the two-region model. The computer program included a non-linear least squares estimation procedure in which the parameters of the distribution, h, K_L and K_R were changed until the variance of the experimental points about the appropriate theoretical relationship was minimal. The parameters associated with the minimum variance were taken as the best value provided by that experiment.

The thickness of the wall boundary region was determined in a similar set of numerical experiments by finding the thickness that corresponded to the minimum variance when the three transport parameters as well as the region thickness were varied.

In the estimation procedures it was found that the temperature profiles were not sensitive to the coefficient of axial dispersion, so that this parameter was allowed to vary between upper and lower limits set in accordance with the principles of Bayes theorem. The temperature profiles were sensitive to the model parameters h and K_R, and α and K_R.

DISCUSSION

Of the four beds under study it was found that the fixed beds of glass and nickel spheres were equally well described by both models, However, the fixed beds of plastic spheres were generally better described by the two-region model. The details of parameters and variances for experiments with polypropylene spheres are given in Table 1.

The mean variance for Model 2 is one third of that found for Model 1, and although there is some scatter in the radial Peclet group it is evident that this group is about 20 for Model 1 (the upper band) but half as much, with an average value of 10 for Model 2. The wall Nusselt numbers, however, agree fairly well for both models.

Figure 3 is a typical comparison of temperature profiles for the two models at three Reynolds numbers in the range 600–1400. The full lines represent the predictions of Model 2 in which the temperature profile and the temperature gradient are continuous from the centre of the bed to the wall temperature. The dotted profiles represent the predictions of Model 1 showing the discontinuity in temperature at the wall.

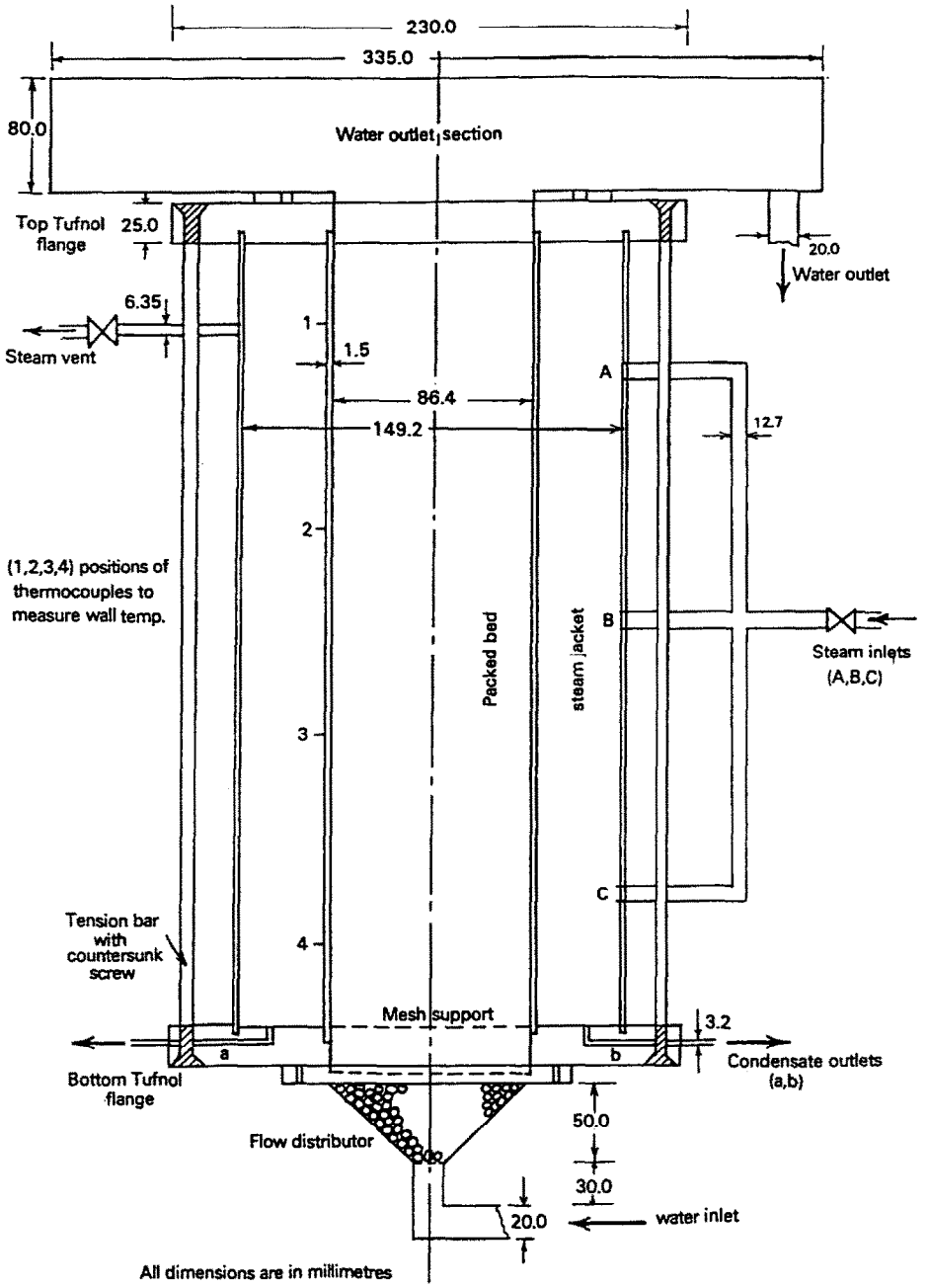

FIG. 2. Experimental arrangement for heat exchanger.

The temperature profiles arising from Model 2 are superior mainly because the relative points cannot be successfully accommodated to Model 1. For the smaller particles for which experiment and the theory are compared in Figs. 4 and 5, Model 2 and Model 1 give equally good representations of the experimental data.

For particles of greater thermal conductivity and smaller size examined in the experiments, differences between the models were small, experimental variances and parameter values were therefore similar for each model. But the combination of large relative size and low thermal conductivity for the polypropylene spheres ensured that the variation of thermal properties near the wall was projected far enough into the bed for significant differences between the two models to be shown at the position of the outer array of sensors.

The differences between the two models is not simply a matter of the magnitude of the variance. The value of the radial Peclet group for mass dispersion in beds of impermeable spheres for the range of Reynolds number covered by the polypropylene sphere experiments is 11 [5]. The analogue between mass

Table 1. Comparison of one- and two-region models for heat transfer to polypropylene spheres, $R_0 - R_1 = 0.02d$

Particle Reynolds number, $dU\rho/\mu$	Model 1 Radial Peclet number, $Ud\rho c/K_R$	Model 1 Nusselt number, hd/λ	Model 1 Variance	Model 2 Radial Peclet number	Model 2 Nusselt number	Model 2 Variance
295	15.9	73	2.7×10^{-5}	6.3	75	5.1×10^{-6}
361	20	74	8.7×10^{-4}	20	53	4.7×10^{-4}
469	20	68	4.8×10^{-4}	18.7	54	8.1×10^{-6}
560	20	78	2.7×10^{-4}	4.9	128	1.2×10^{-4}
614	20	76	4.5×10^{-4}	5.7	282	1.2×10^{-4}
758	18.2	78	4.6×10^{-4}	5.9	60	1.6×10^{-4}
902	19.9	90	4.0×10^{-4}	12.0	67	8.9×10^{-5}
1047	20	91	5.1×10^{-4}	11.1	71	1.3×10^{-4}
1191	18.3	91	8.3×10^{-4}	6.1	69	1.9×10^{-4}
1336	18.2	92	7.3×10^{-4}	6.8	74	2.0×10^{-4}
1480	20	102	5.7×10^{-4}	7.3	76	2.3×10^{-4}
1661	20	100	7.1×10^{-4}	12.4	77.5	3.3×10^{-4}
Mean			5.20×10^{-4}			1.72×10^{-4}

radial dispersion and radial dispersion and radial dispersion of heat in beds of impermeable spheres is the equality between the corresponding Peclet groups. Therefore, as all spheres are permeable to heat a Peclet group of 11 for radial dispersion of heat is an upper bound since radial flow of heat through the particles will cause a reduction in Peclet group below 11. At high Reynolds number when the convective element of radial dispersion is dominant, the value of radial Peclet groups for thermal disperion will also be 11. Thus the values of radial Peclet groups of 20 shown in Table 1 for Model 1 are not feasible.

Model 2 is therefore to be preferred. The agreement of both parameters and variance for both models when the particles are small or of high thermal conductivity is significant. When the particles are small the temperature discontinuity for Model 1 and the temperature change in the wall region for Model 2 both represent a small element of the total temperature distribution. When the particles are larger the idealization of the wall boundary region as a temperature discontinuity at the wall becomes less satisfactory, a criticism of Model 1 that is met by Model 2. Model 2 is appropriate when the ratio of tube to particle diameter is small, while Model 1 is appropriate when this ratio is large. The dual nature of the models is clearly an important feature that allows the results of experiments that have previously been interpreted by Model 1 to be incorporated into the structure of model 2.

In addition to the comparison of models the other significant results of this investigation are the dependences of the radial Peclet group and the wall Nusselt number upon Reynolds numbers from 5 to 1660 and for glass, polypropylene and nickel spheres. The dependence of Peclet group upon Reynolds number is shown in Fig. 6. The experimental results for Model 1 and Model 2 are distinguished only for the polypropylene spheres since for these experiments only were there significant differences between the two models: the unacceptable feature of the results from Model 1 is the value of 20 for the radial Peclet group, twice the value of estimates from Model 2 and twice the maximum value estimated from analogous experiments on mass dispersion.

There was possible evidence of a small effect of natural convection upon heat transfer to intermediate size particles. Takata *et al.* [6] have presented a numerical analysis of heat transfer by natural convection without net flow in a porous medium enclosed by concentric circular cylinders at different inclinations to the horizontal. They presented these results as the dependence of a Nusselt group defined as the ratio of, radial thermal conduction with natural convection/radial conduction without, upon the product of the Rayleigh and Darcy groups defined as

$$\left(\frac{g\beta\Delta T h^3}{\alpha_m \nu}\right)\left(\frac{k}{h^2}\right)$$

(g is the acceleration due to gravity, β the coefficient of volumetric expansion, ΔT the temperature difference, h the height, k the permeability, α_m the thermal diffusivity for the medium, and ν is the dynamic viscosity). If ΔT is taken to be the difference between the wall and the mid bed temperatures, the value of the product of the Rayleigh and Darcy groups was about 50. The calculations of Takata *et al.* indicate that for natural convection, an enhancement in heat transfer of about 10% would be expected. It is apparent from Fig. 6 that there is a trend of results for 6 mm particles just below equation (9) and this small difference may be due to enhancement of heat transfer by natural convection, but the enhancement is evidently less than 10%.

Except for the experiments on 0.5 mm diameter glass spheres dispersion was mainly dominated by convection [5], although the influence of radial conduction through the particle phase can be seen in the arrangement of experimental results into bands with

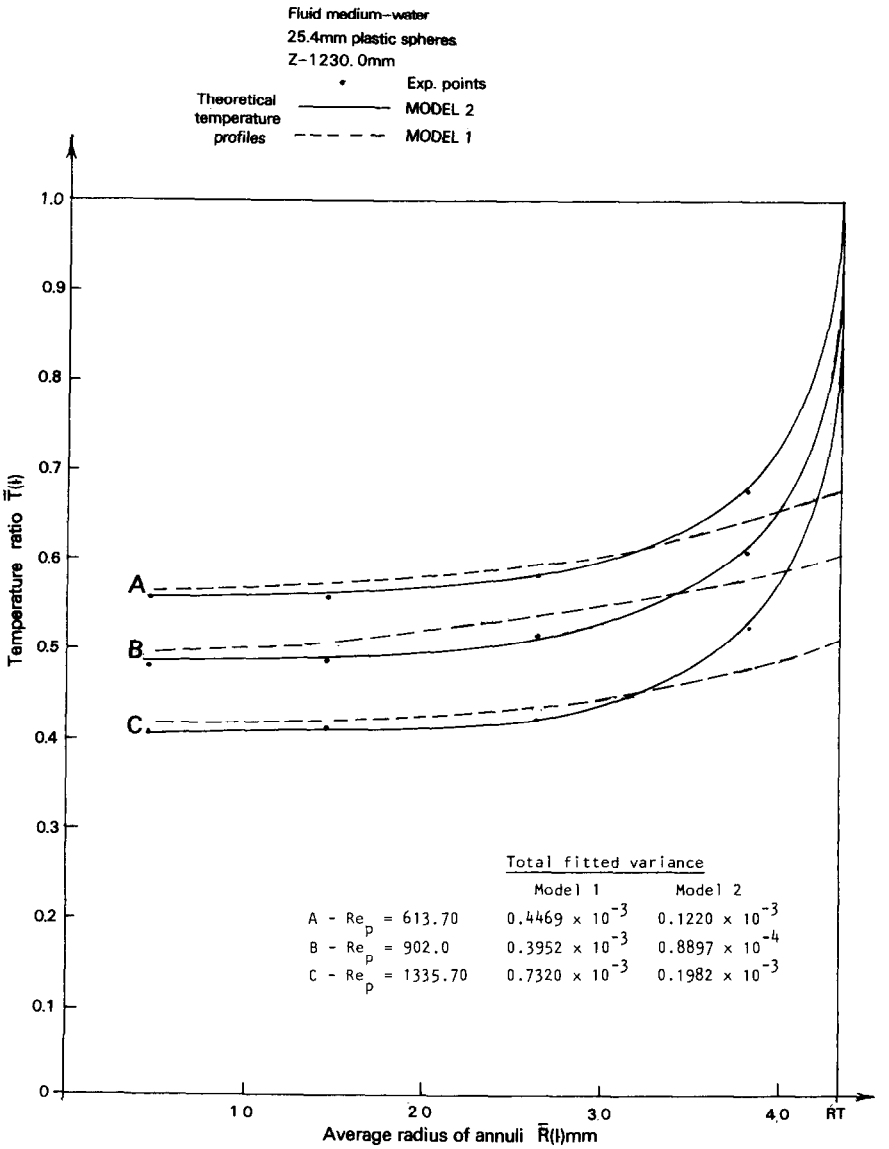

FIG. 3. Comparison of temperature profiles for experiments on polypropylene spheres at three different Reynolds numbers. The full lines correspond to Model 2 and the dotted lines to Model 1.

results for polypropylene spheres showing the greater Peclet group, and those for nickel spheres the least.

The significant influence of molecular or thermal conduction can be seen only for 0.5 mm glass spheres. There is a particular point of interest because the thermal conductivity of water and of glass are similar with handbook values for the thermal conductivity of soda glass in the range of 0.7–0.9 and of water in the range of 0.54–0.76 W m^{-1} K^{-1} for 0–100°C.

As the experimental results for the 0.5 mm diameter particles suggest, the Peclet group at low Reynolds number is directly proportional to Reynolds number because the coefficient of thermal dispersion becomes constant at low Re. If λ_0 is the value of K_R at low Reynolds number, it should be approximately equal to the thermal conductivity of water. In an analysis of radial dispersion of mass it has been shown [5] that the diffusive and convective contributions to dispersion are independent, and by analogy for heat, the diffusive components of solid and fluid are independent of the convective contribution. Since the components are independent, if dispersion is considered to be a stochastic process with random displacements, the total variance of the stochastic motion is the sum of the diffusive and convective motions. Then the total coefficient is the sum of the convective and diffusive coefficients

$$K_R = K_{Rf} + \lambda_0 \tag{8}$$

or in terms of the Peclet group

$$\frac{1}{Pe} = \frac{1}{Pe_f} + \frac{\lambda_0}{\lambda\, Re\, Pr} \tag{9}$$

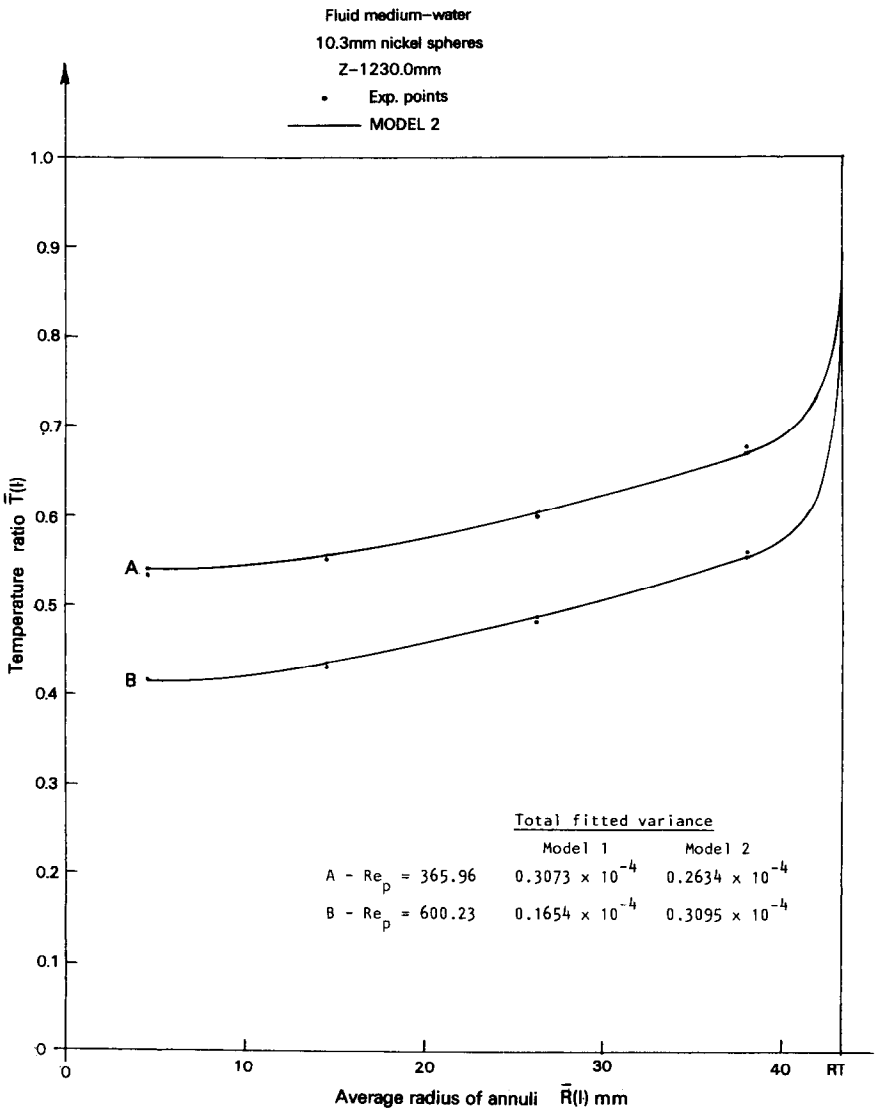

FIG. 4. Comparison of temperature profiles for experiments on nickel spheres with prediction of Model 2.

where Pe_f if a function of Reynolds number alone. For fixed beds of spheres Pe_f is given by [7]

$$Pe_f = 40 - 29\exp(-7/Re). \quad (10)$$

Equation (9) with $\lambda_0 = \lambda$ is plotted as a solid line on Fig. 6 and shows good agreement with the experimental results for glass particles. The sharp decline of Peclet group predicted by equation (9) occur at a Reynolds number just smaller than the lowest values attained in this investigation. However, within the range of experiments agreement between experiment and equation (9) is within experimental error taking into account the uncertainties of thermal conductivities of fluid and solid due to variations in temperature across the bed.

The other model parameter of importance is the Nusselt group and the dependence of this group upon Reynolds number is shown in Fig. 7, where the legend is the same as that employed for Fig. 6.

At low Reynolds number the temperature difference at the wall, or across the wall region is small because the particles are only 0.5 mm in diameter in a tube of 88 mm diameter, so that there is a larger degree of experimental variation. As the Reynolds number increases, there is a corresponding increase of Nusselt number.

Stock and Coeuret [8] have examined experimental measurements of mass transfer from a wall into fixed beds of spheres. The most accurate estimates of the wall Sherwood group have been provided by the electrochemical method for the determination of mass transfer rates in which limiting current measurements are made to determine the rate of mass transfer between a large anode and a small cathode. The small size of the cathode and the speed of the electrochemical reaction ensure that the limiting rate is determined by mass transfer resistance in the vicinity of the wall. The results of four independent experimental investigations may be correlated by the expression

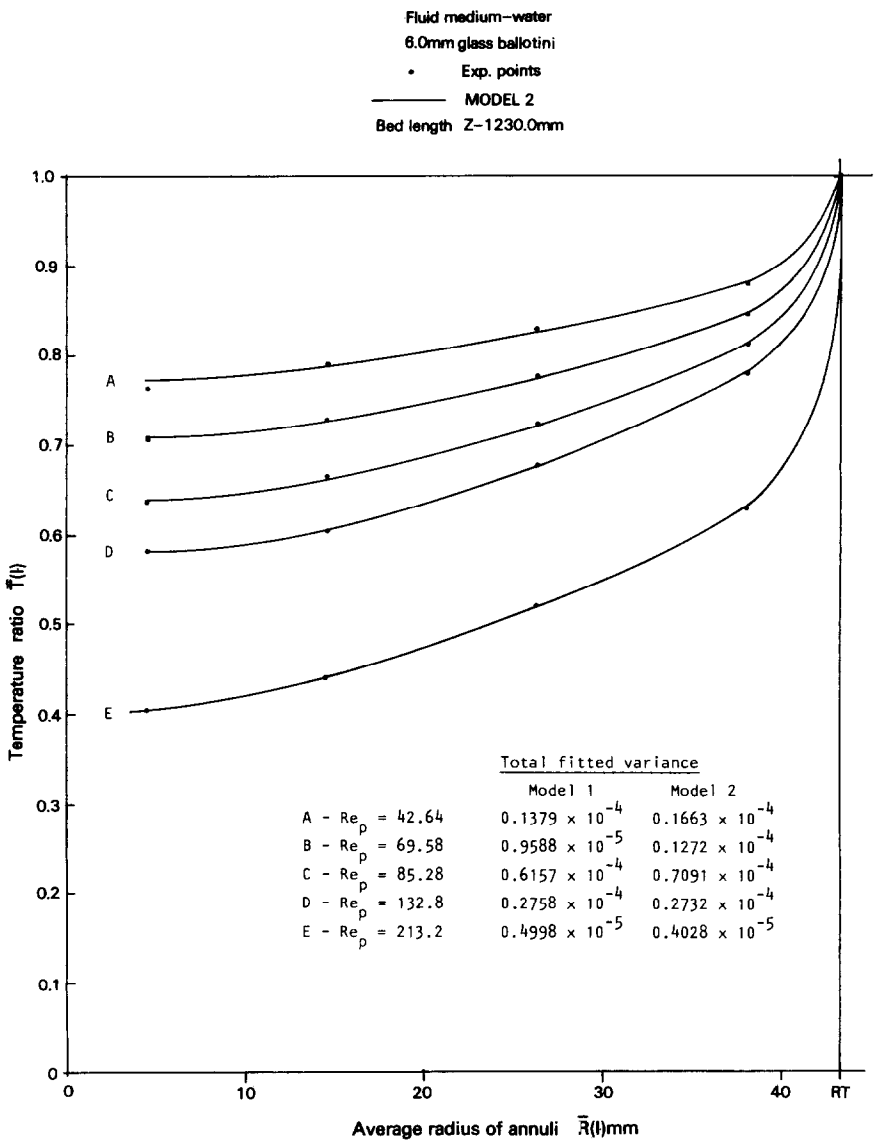

FIG. 5. Comparison of temperature profiles for the experiments on glass spheres with prediction of Model 2.

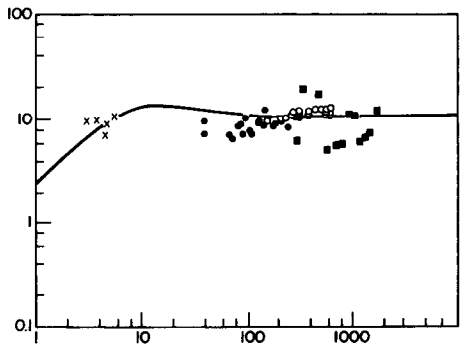

FIG. 6. The experimental dependence of Peclet group upon Reynolds number: ×, 0.5 mm diameter glass spheres; ●, 6 mm diameter glass spheres; ○, 10 mm diameter nickel spheres; ■, 25 mm diameter polypropylene spheres. The full line corresponds to equation (9).

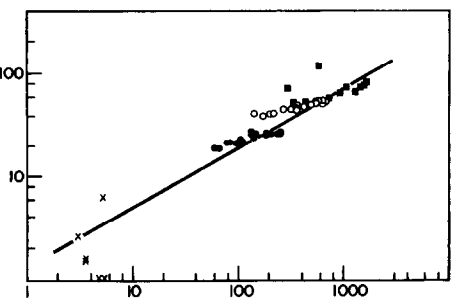

FIG. 7. The experimental dependence of wall Nusselt number upon Reynolds number: ×, 0.5 mm diameter glass spheres; ●, 6 mm diameter glass spheres; ○, 10 mm diameter nickel spheres; ■, 25 mm diameter polypropylene spheres. The full line corresponds to equation (12).

$$Sh = 0.8Sc^{1/3}\,Re^{0.6}. \quad (11)$$

If the predominant heat transmission path is through the fluid phase, the heat transfer group analogous to equation (11) is simply

$$Nu = 0.8Pr^{1/3}\,Re^{0.6}. \quad (12)$$

This equation is plotted as the solid line of Fig. 7, and is a good representation of the dependence of experimental Nusselt group upon the Reynolds number. The agreement suggests that the contribution of the solid phase to the thermal transmittance of the wall region is small. This finding is consistent with the experimental estimates of thermal dispersion in that the regimes of both dispersion and wall transmittance are dominated by convection rather than molecular conduction in the experimental range covered by this investigation.

REFERENCES

1. D. J. Gunn and M. Khalid, Thermal dispersion and wall heat transfer in packed beds, *Chem. Engng Sci.* **30,** 261 (1975).
2. L. M. S. Roblee, R. M. Baird and J. W. Tierney, Radial porosity variations in packed beds, *A.I.Ch.E. Jl* **4,** 460 (1958).
3. J. Schuster and D. Vortmeyer, Ein einfaches Verfahren zur näherungsweisen Bestimmung der Porosität in Schuttungen als Funktion des Wandabstandes, *Chem. Eng. Technik* **52,** 848 (1980).
4. D. J. Gunn and M. M. Ahmad, The characterisation of radial heat transfer in fixed beds, *I. Chem. E. Symp. Ser.* **86,** 513–520 (1984).
5. D. J. Gunn, Theory of axial and radial dispersion in packed beds, *Trans. Instn Chem. Engrs* **47,** 351 (1969).
6. Y. Takata, K. Fukuda, S. Hosegawa, K. Iwashige, H. Shimaura and K. Sanokawa, Three dimensional natural convection in a porous medium enclosed with concentric inclined cylinders, *Proc. Seventh Int. Heat Transfer Conference*, Munich, Vol. 2, pp. 351–356 (1982).
7. D. J. Gunn, Axial and radial dispersion in fixed beds, *Chem. Engng Sci.* **42,** 363 (1987).
8. A. Stock and F. Coeuret, Mass transfer between a flowing liquid and a wall or an immersed surface in fixed and fluidised beds, *Chem. Engng J.* **20,** 149 (1980).

UN MODELE DISTRIBUE POUR LE TRANSFERT THERMIQUE EN PHASE LIQUIDE DANS DES LITS FIXES

Résumé—Bien que la représentation du transfert thermique en phase gazeuse par des modèles distribués est maintenant établie, il n'a pas été traité de ces modèles en phase liquide. Dans le cas étudié ici, le liquide en écoulement dans un lit fixe de particules est chauffé à la paroi du lit et la distribution de température est mesurée à la sortie du lit par un arrangement de thermocouples. La distribution expérimentale de température est comparée avec la distribution calculée par deux modèles. Dans le premier modèle, le transfert thermique est supposé se faire par une dispersion thermique radiale et axiale et un transport axial, avec une résistance thermique à la paroi pour représenter les changements de porosité et de conductivité près de la paroi. Dans le second modèle, on garde la même description dans le noyau central, mais on considère une variation des propriétés thermiques près de la paroi, sur une fraction de diamètre de particule. Pour des petites particules et des particules à grande conductivité thermique les deux modèles représentent les données expérimentales également bien dans le domaine de nombre de Reynolds depuis 5 jusqu'à 1000. Pour les grandes particules à faible conductivité thermique, le modèle à deux zones donne une représentation plus satisfaisante que l'autre des mesures expérimentales.

EIN RECHENMODELL MIT VERTEILTEN PARAMETERN FÜR DIE WÄRMEÜBERTRAGUNG AN FLÜSSIGKEITEN IN FESTBETTEN

Zusammenfassung—Obwohl die Wärmeübertragung in der Gasphase nun mit Rechenmodellen mit verteilten Parametern beschrieben werden kann, wurde über entsprechende Untersuchungen für die Flüssig-Phase bisher nichts bekannt. Diese Arbeit handelt von Untersuchungen, bei denen Flüssigkeit, die durch ein Festbett aus Partikeln fließt, an der Wand der Schüttung aufgeheizt und die Temperaturverteilung am Ende der Schüttung mit einer Reihe von Themoelementen gemessen wurde. Die experimentell ermittelte Temperaturverteilung wurde mit der nach zwei unterschiedlichen Modellen berechneten verglichen. Im ersten Modell wurde Wärmeübertragung durch radiale und axiale thermische Dispersion sowie axiale Konvektion angenommen, wobei Abweichungen der Porosität und der Wärmeleitfähigkeit in Wandnähe durch einen Wärmeleitwiderstand an der Wand dargestellt wurden. Im zweiten Modell wurde für den Kernbereich das gleiche Wärmeübertragungsmodell angewandt, für eine Wandgrenzschicht (ein Bruchteil eines Partikeldurchmessers) wurde jedoch eine Variation der thermischen Stoffeigenschaften angenommen. Für die Wärmeübertragung an kleine Partikel und an Partikel mit hoher Wärmeleitfähigkeit näherten sich beide Modelle in einem Bereich der Reynolds-Zahl von 5 bis 1000 den Meßwerten mit gleich großer Genauigkeit an. Bei großen Partikeln mit niedriger Wärmeleitfähigkeit erreichte das 2-Zonen-Rechenmodell jedoch eine bedeutend bessere Annäherung an die Meßwerte.

ДИСТРИБУТИВНАЯ МОДЕЛЬ ТЕПЛООБМЕНА В ПЛОТНОМ СЛОЕ С ЖИДКОЙ ФАЗОЙ

Аннотация—Теплообмен в плотном слое с газовой фазой уже давно описывается с помощью дистрибутивных моделей, однако, до сих пор отсутствует соответствующая проверка их применимости к описанию теплообмена в слое с жидкой фазой. В настоящей статье рассматривается случай, когда фильтрующаяся через неподвижные слои частиц жидкость нагревается у стенки слоя, а распределение температур находится по показаниям термопар на выходе из слоя. Экспериментально определённое распределение температур сравнивается с распределением температур, найденным по двум моделям теплообмена в неподвижном слое. В первой модели предполагалось, что имеет место поперечное (радиальное) и продольно-осевое рассеяние тепла, а осевая конвекция с термическим сопротивлением на стенке использована для описания изменения порозности и теплопроводности у стенки. Согласно второй модели теплообмен в объёме слоя рассчитывался аналогичным образом, а в области, отстающей от стенки на долю диаметра частиц, учитывалось изменение свойств. В диапазоне чисел $Re = 5$–1000 обе модели одинаково хорошо описывают экспериментальные данные по теплообмену в слое из мелких частиц и частиц с высокой теплопроводностью. Однако для слоя из крупных частиц с низкой теплопроводностью двухзонная модель даёт гораздо лучшую сходимость с экспериментальными данными.